Chinese Herbal Medicines 11 (2019) 60–69

Contents lists available at ScienceDirect

Chinese Herbal Medicines

journal homepage: www.elsevier.com/locate/chmed

Original Article

Screening potential α-glucosidase inhibitors from *Anemarrhena asphodeloides* using response surface methodology coupled with grey relational analysis

Tian-cheng Ma, Yu Sun*, Li-na Guo, Lei Liu, Zhen-yan Liu, Yu-mei Wang, Song-jie Fan

Research Institute of Medicine and Pharmacy, Qiqihar Medical University, 161006 Qiqihar, China

ARTICLE INFO

Article history:
Received 1 April 2017
Revised 27 June 2018
Accepted 12 August 2018
Available online 12 October 2018

Keywords:
Anemarrhena asphodeloides Bge.
α-glucosidase inhibitory activities
grey relational analysis
response surface methodology
UPLC-Q-TOF-MS

ABSTRACT

Objective: To screen potential α-glucosidase inhibitors from *Anemarrhena asphodeloides*.
Methods: Response surface methodology employing Box-Behnken design was used to optimize conditions for the extraction of α-glucosidase inhibitory active compounds from *A. asphodeloides*. The powders (20.0 g) of *A. asphodeloides* were extracted under the optimized conditions. The extract was applied to a D-101 macroporous resin column. It was eluted with ethanol and water to give six fractions. Compounds from the active fraction were identified by UPLC-Q-TOF-MS. The structure-activity relationship was discussed based on grey relational analysis.
Results: The optimum extraction conditions were as follows: ethanol concentration, 100%; extraction temperature, 51 °C; and solvent to solid ratio, 23 mL/g. It indicated that the active compounds were concentrated into 80% ethanol fraction. Twenty five steroid saponins from 80% ethanol fraction were identified by UPLC-Q-TOF-MS. Peaks 19 and 23 were tentatively identified as new structures. The predicted α-glucosidase inhibitory activities of the compounds were **7** > **2** > **1** > **22** > **23** > **3** > **9** > **21** > **24** > **4** > **13** > **8** > **14** > **16** > **17** > **25** > **6** > **19**.
Conclusion: The fraction eluted by 80% ethanol showed the best inhibitory activity. After analyzing the data of UPLC-Q-TOF-MS, 25 steroid saponins were tentatively identified in this fraction.

1. Introduction

Diabetes mellitus is a persistent disease. It is identified by increasing blood glucose levels due to derangement in the carbohydrate, protein, and fat metabolism (Joseph & Jini, 2011). α-Glucosidase (EC. 3.2.1.20) is located on the brush border membrane of the small intestine (Hirsh, Yao, Young, & Cheeseman, 1997). It plays a significant role in catalyzing the hydrolysis of glycosidic bond ($\alpha_{1\text{-}4}$), which results in the release of free glucose into the digestive tract (Wang, Peng, Wang, Li, & Li, 2016). α-Glucosidase inhibitors could decrease the absorption of carbohydrates from the digestive tract and reduce after-meal glucose levels (Nhiem et al., 2010). α-Glucosidase inhibitors like Acarbose, Miglitol and Voglibose have been applied in clinical for the treatment of type 2 diabetes mellitus (Martin & Montgomery, 1996; Toeller, 1994). However, the synthetic hypoglycemic agents often cause severe gastrointestinal side effects (Zhou et al., 2015). Therefore, there is a great need for natural α-glucosidase inhibitors derived from Chinese materia medica.

Anemarrhena asphodeloides Bge. belongs to the family Liliaceae. It is widely distributed in China (Zhao et al., 2013). Phytochemical studies have identified several classes of components such as steroidal saponins, flavonoids, xanthones, anthraquinones, phenylpropanoids, alkaloids, and organic acids (Ji & Feng 2010; Youn et al., 2009). The rhizomes of *A. asphodeloides* have been reported to have α-glucosidase inhibitory activities relevant to treatment of diabetes mellitus (Dou et al., 2013; Ichiki et al., 2007; Nian, Li, Liu, & Li, 2017). Steroids are the main active components of *A. asphodeloides*. They have extremely diverse structures with a broad spectrum of pharmacological and biological activities (Kang et al., 2011; Lee, Jung, & Kim, 2009; Wang et al., 2002, 2013). Particular attention has been focused on their potential for α-glucosidase inhibitory activities (Khang, Phuong, & Ma, 2017).

Ultra performance liquid chromatography coupled with mass spectrometry (UPLC-MS) has a pronounced capability for identification of structures. Q-TOF-MS is a powerful technique for the compound identification in which the exact mass of the compounds can be tested and a unique elemental formula based on the

* Corresponding author.
E-mail address: zsy5811321@126.com (Y. Sun).

https://doi.org/10.1016/j.chmed.2018.08.010
1674-6384/

constituent atoms can also be acquired (Wang, Qi, Zhang, & Yuan, 2014). Response surface methodology (RSM) has been widely used in analyzing a variety of biological processes, designing the experiment, building models, evaluating the effects of different factors, and optimizing conditions (Oh, Rheem, Sim, Kim, & Baek, 1995; Sun, Gao, Zhao, & Cheng, 2013). It dramatically reduces the number of experiment required to evaluate the effect of the variables on the interactions and responses (Yang, Yu, & Hwang, 2003). Grey relational analysis (GRA) is also called Deng's Grey Incidence Analysis model. It is one of the most widely employed models of Grey system theory (Xu et al., 2011). It has been applied to evaluate the significance of the influencing factors in complex biological processes. It qualitatively and quantitatively explains the interrelationships between multiple factors and variables with minimal information needed (Xu et al., 2013).

As part of our ongoing focus on the discovery of new active agents from *A. asphodeloides* (Sun, Li et al., 2014; Sun, Peng et al. 2014; Sun et al., 2015, 2016), we are interested in α-glucosidase inhibitory activities of steroid saponins from *A. asphodeloides*. In this paper, optimization of extraction temperature, ethanol concentration, and solvent to solid ratio were investigated. The best extraction condition of α-glucosidase inhibitory activities from *A. asphodeloides* using RSM combined with Box-Behnken design (BBD) was tested. *A. asphodeloides* extracted with the optimized extraction method was applied to a D-101 macroporous resin column. It eluted with ethanol and water to produce 0%, 20%, 40%, 60%, 80%, and 100% ethanol fractions. Then they were tested on α-glucosidase inhibitory activities. It indicated that the extract was divided into six fractions and active compounds were gathered into 80% ethanol fraction. A total of 25 saponins from the 80% ethanol fraction were identified and tentatively characterized by LC-TOF-MS. GRA was employed to evaluate the relationship between the structures of the compounds and α-glucosidase inhibitory activities.

2. Materials and methods

2.1. Plant material

The rhizomes of *A. asphodeloides* were purchased from Beijing Tongrentang Pharmacy. The plant materials were identified by Prof. Lina Guo from Research Institute of Medicine and Pharmacy, Qiqihar Medical University.

2.2. Chemicals and reagents

α-Glucosidase and *p*-nitrophenylalpha-D-glucopyranoside (PNPG) were purchased from Sigma Company. Acarbose was purchased from Shanghai Yuanju Bio-Technology Ltd. Timosaponin AIII, timosaponin BII, anemarrhenasaponin III, timosaponin G and anemarrhenasaponin I were prepared by ourselves. Acetonitrile was purchased from Merck Company. Sulfuric acid, methanol, and ethanol were purchased from Tianjin Fuyu Chemical Co., Ltd. Formic acid, sodium carbonate, and phosphate were purchased from Tianjin Commie Chemical Reagent Co., Ltd.

2.3. Extraction procedure

Dried rhizomes of *A. asphodeloides* were powdered by a disintegrator and then sieved into a homogeneous size (60 mesh). Extractions were carried out in water baths. The powders of 2.0 g were soaked in different proportions of ethanol-water (from 0% to 100%, from 20 mL to 100 mL). Then, the heated reflux extraction experiments were conducted in water baths (from 40 °C to 100 °C) for 1 h.

2.4. Separation procedure

The powder (20.0 g) of *A. asphodeloides* was extracted under the optimized conditions. The extract was applied to a D-101 macroporous resin column. It eluted with ethanol and water to afford 0%, 20%, 40%, 60%, 80%, and 100% ethanol fractions.

2.5. α-glucosidase inhibition assay

According to the modified method of previous report (Wang et al., 2016), the inhibitory activities of α-glucosidase were tested. A total of α-glucosidase (20 μL, 1 U/mL in PBS, pH 6.8), and the sample solution (20 μL) were placed in a 96-well microplate, then incubated for 15 min at 37 °C. PNPG (2.5 mmol/L, 20 μL) was added and the mixture was incubated additionally for 15 min at 37 °C. After this time, 0.2 mol/L Na_2CO_3 (80 μL) was added to the mixture. The absorbance of each well was measured at 405 nm with a microplate spectrophotometer. Each analyte was tested for three times, and an average value was applied. Mixtures with PBS instead of PNPG were set as controls. Acarbose was used as the positive control.

2.6. Contents of steroid saponins assay

Stock solution of timosaponin AIII was prepared in methanol at concentration of 0.128 mg/mL. A set of timosaponin AIII standard solutions were obtained by adding different volumes of stock solution with 0.1, 0.2, 0.4, 0.8, 1, 2, and 5 mL to test tubes. Then evaporated the solutions to dryness. Sulfuric acid (2 mL) was added and the mixture was incubated for 30 min at 80 °C. After this time, methanol (8 mL) was added and incubated for 30 min at 0 °C. The absorbance of the solution was read at 321 nm using ultraviolet spectrophotometer. Different standard solutions were used to prepare a calibration curve. Results were expressed as milligram timosaponin AIII equivalents/g *A. asphodeloides*.

2.7. Identification of active fraction and structure characterization

The constituents of the fractions were assayed by UPLC-Q-TOF-MS. UPLC system (Shimadzu, Japan) consisted of a model LC-30AD pump and a model SIL-30AC Autosampler. The chromatograph was equipped with a gradient mobile phase. Mobile phases were water with 0.1% of formic acid (A) and acetonitrile with 0.1% of formic acid (B). The gradient used was as follows: 0.01 min, 20% B; 0.01–1 min, 20% to 30% B; 1–7 min, 30% to 50% B; 7–10 min, 50% to 70% B; 10–15 min, 70% to 100% B; 15–16 min, 100%; 16–16.1 min, 100% to 20% B; 16.1–18 min, 100% B. The injection volume of sample was 1 μL. The flow rate was 0.3 mL/min and the column temperature was 35 °C. The Q-TOF-MS system (AB, America) with an ESI source was performed in positive mode and negative mode. The parameters of ESI-MS were set as follows: Ion Source Gas 1 (50 psi), Ion Source Gas 2 (50 psi), Curtain Gas (35 psi), temperature (500 °C), IonSpray Voltage Floating (5500 V), Declustering Potential (100 V), Collision Energy (10 V). MS conditions were corrected by APCI Positive Calibration Solution for the AB SCIEX Triple TOF™ Systems. The data were analyzed by Analyst TF 1.7.1 Software.

2.8. Responses surface methodology

RSM was employed to determine the optimum levels of extraction temperature (°C) (X_1), ethanol concentration (%) (X_2) and solid-to-liquid ratio (mL/g) (X_3) related to two responses yields of α-glucosidase inhibitory activities and contents of steroid saponins. We evaluated the effects of ambient temperature that varied from 40 °C to 70 °C, ethanol concentration was ranged from 50% to 100%, and the ratio of solvent to solid was evaluated from 10 mL/g

to 30 mL/g. All these conditions were selected based on preliminary experimental results. Moreover, BBD with RSM was applied to identify the best combination of the parameters. The effect of three parameters on the extractions was investigated at three levels (−1, 0, and +1). In total, seventeen experiments were conducted in random order. The values were fitted with a second-order polynomial model given below:

$$Y = \beta_0 + \sum_{i=1}^{3} \beta_i X_i + \sum_{i=1}^{3} \beta_{ii} X_i^2 + \sum_{i=1}^{3} \sum_{j=i+1}^{3} \beta_{ij} X_i X_j$$

Where Y was the response; X_i and X_j were the independent variables influencing the response Y; β_0, β_i, β_{ii}, and β_{ij} described the regression coefficients for intercept, linear, quadratic and interaction terms, respectively. Design-Expert 8.0.6 was used to statistically analyzed the data obtained from the BBD for the optimization of the experiments. The quality of fit of the polynomial models was evaluated with respect to the coefficient of determination (R^2) and F-test. The lack of fit F-value ($P < 0.05$) was acquired by analysis of variance (ANOVA) and used to demonstrate variable significance and model adequacy.

2.9. Gray relative analysis

GRA was carried out to evaluate the relationship between constituents of *A. asphodeloides* and α-glucosidase inhibitory activities. GRA was performed by the following steps:

Normalization treatment of raw data: Lower IC_{50} value showed better α-glucosidase inhibitory activities. The raw data should make reciprocal transformation before normalization treatment. The data processing was conducted under the instruction of literature (Li, Li, He, Ma, & Ma, 2014). Then we supposed that there were n samples and each sample had m indexes. The X_0 was the desired sequence and the evaluation unit sequence was X_i. The raw data was normalized by the mean numerical calculation method.

$$X_{i'}'(k) = X_i(k) / \frac{1}{m} \sum\nolimits_{j=1}^{m} X_j(k)$$

Calculation of the correlation coefficient: the correlation coefficient reveals the accordance between the desired sequence and the evaluation unit sequence. The greater value of correlation coefficient indicates that the evaluation unit sequence is closer to desired sequence. The calculation formula of correlation coefficient was as follow:

$$\varepsilon_i(k) = \frac{\min\limits_i \min\limits_k |X_0(k) - X_i(k)| + \rho \max\limits_i \max\limits_k |X_0(k) - X_i(k)|}{|X_0(k) - X_i(k)| + \rho \max\limits_i \max\limits_k |X_0(k) - X_i(k)|}$$

$\rho = 0.5$, $\max\limits_i \max\limits_k |X_0(k) - X_i(k)|$ was the secondary minimum differential value and $\min\limits_i \min\limits_k |X_0(k) - X_i(k)|$ was the secondary maximum differential value.

Calculation of the correlation degree and weight value: too much correlation coefficients and the dispersive information make it inconvenient to compare the data. It is a great need to concentrate the correlation coefficient into a value. According to the correlation degree (r_i), the weight value of evaluated samples can be normalized. The formula of correlation degree was:

$$r_i = \frac{1}{N} \sum_{k=1}^{N} \varepsilon_i(k)$$

3. Results

3.1. Single-factor experiments

3.1.1. Effect of extraction temperature

The effect of extraction temperature with different temperature (from 40 °C to 100 °C) were tested for the extraction of α-glucosidase inhibitory activities. The results were presented in Fig. 1A. The α-glucosidase inhibitory activities of extracts increased with the increase of extraction temperature from 40 °C to 55 °C. However, the activities of extracts decreased with the increase of extraction temperature from 55 °C to 85 °C. On the basis of these results, the extraction temperature of 40, 55, and 70 °C were chosen for the following tests.

3.1.2. Effect of ethanol concentration

Choice of a proper solvent is very important to guarantee the extraction of active compounds. The extractions were performed with different amount of ethanol ranging from 0% to 100%. The results were shown in Fig. 1B. Higher ethanol concentration tended to favor α-glucosidase inhibitory activities of extracts. The from 50% to 100% were selected for the following tests.

3.1.3. Effect of liquid/solid ratio

To increase the extraction efficiency and decrease the solvent consumption, the liquid/solid ratio was optimized. The results were shown in Fig. 1C. Considering the results and solvent consumption, liquid/solid ratios from 10:1 to 30:1 (mL/g) were used for the following tests.

3.2. Optimization of extractions using BBD

In order to optimize the extraction conditions, BBD combined with RSM was utilized. The operating conditions and experiment data were shown in Table 1. These data were analyzed using Design Expert 8.0.6 Software for second-order polynomial regression analysis and ANOVA. This mathematical regression model was shown below in terms of coded where Y_1 and Y_2 were α-glucosidase inhibitory activities and the contents of steroid saponins.

The relationship between α-glucosidase inhibitory activities and the extraction parameters (coded factors) was given below:

$$Y_1 = 4.17 + 0.88X_1 - 3.20X_2 + 1.02X_3 - 0.36X_1X_2 - 0.018X_1X_3 - 1.16X_2X_3 + 1.02X_1^2 + 0.030X_2^2 + 0.61X_3^2$$

The relationship between the contents of steroid saponins and the extraction parameters (coded factors) was shown below:

$$Y_2 = 64.16 + 0.76X_1 - 14.02X_2 - 4.91X_3 - 1.19X_1X_2 + 0.093X_1X_3 + 1.31X_2X_3 - 0.80X_1^2 + 0.51X_2^2 + 1.32X_3^2$$

ANOVA of the experimental data (Table 2) showed correlation coefficient of determination values for α-glucosidase inhibitory activities and the contents of steroid saponins. This indicated that this model was applicable to describe the response of the experiment pertaining to the inhibitory activities of α-glucosidase and the contents of steroid saponins.

RSM was regarded as one of the best way to visualize the influence of the independent variables on the dependent ones. Fig. 2 showed 3D plots of the response surface for the inhibitory activities of α-glucosidase and the contents of steroid saponins as related to the extraction temperature, ethanol concentration, and liquid/solid ratio. The inhibitory activities of α-glucosidase increased significantly with increasing ethanol concentration. Increasing the

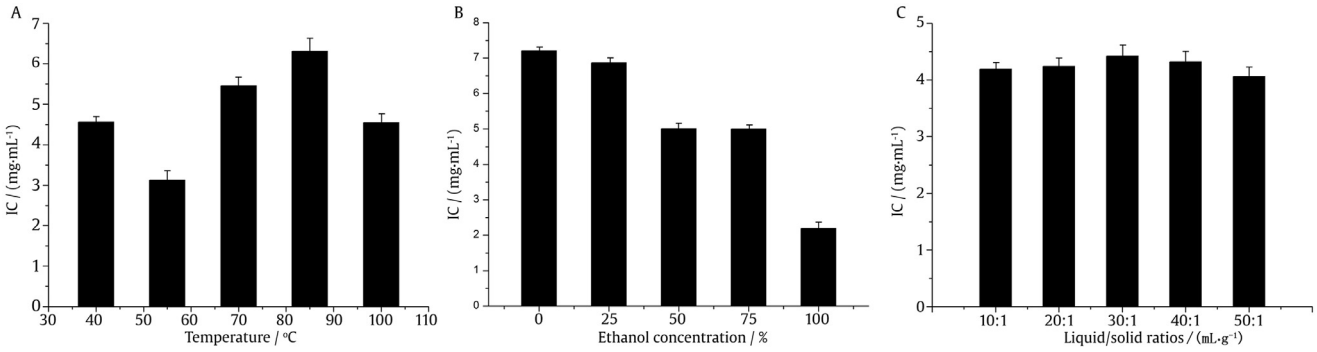

Fig. 1. Effects of temperature (A), ethanol concentration (B), and liquid/solid ratio (C) on α-glucosidase inhibition activities of extracts.

Table 1
Experimental design applied to extraction and responses of α-glucosidase inhibition activities and contents of steroid saponins in BBD assays.

Runs	Independent variables			Responses	
	extraction temperature / °C	ethanol concentration / %	solid-to-liquid ratio / (mL·g^{-1})	α-glucosidase inhibition activities / (mg·mL^{-1})	contents of steroid saponins/(mg·g^{-1})
1	40 (−1)	50 (−1)	20 (0)	7.13	76.02
2	70 (1)	50 (−1)	20 (0)	9.73	78.02
3	40 (−1)	100 (1)	20 (0)	1.43	52.10
4	70 (1)	100 (1)	20 (0)	2.58	49.33
5	40 (−1)	75 (0)	10 (−1)	4.04	69.95
6	70 (1)	75 (0)	10 (−1)	5.73	73.20
7	40 (−1)	75 (0)	30 (1)	5.91	55.98
8	70 (1)	75 (0)	30 (1)	7.53	59.60
9	55 (0)	50 (−1)	10 (−1)	5.72	85.10
10	55 (0)	100 (1)	10 (−1)	1.65	52.71
11	55 (0)	50 (−1)	30 (1)	10.29	76.64
12	55 (0)	100 (1)	30 (1)	1.58	49.49
13	55 (0)	75 (0)	20 (0)	4.08	66.63
14	55 (0)	75 (0)	20 (0)	4.06	62.03
15	55 (0)	75 (0)	20 (0)	4.17	64.43
16	55 (0)	75 (0)	20 (0)	4.29	63.19
17	55 (0)	75 (0)	20 (0)	4.23	64.51

Table 2
Analysis of variance tables for α-glucosidase inhibitory activities and contents of steroid saponins.

Responses	Source of variation	Sum of squares	Df	Mean square	F value	P value Prob > F
α-Glucosidase inhibitory activities	Model	108.94	9	12.10	568.50	< 0.0001
	A-extraction temperature	6.23	1	6.23	292.62	< 0.0001
	B-the ethanol concentration	82.11	1	82.11	3856.45	< 0.0001
	C-solid-to-liquid ratio	8.34	1	8.34	391.86	< 0.0001
	AB	0.53	1	0.53	24.69	0.0016
	AC	1.23×10^{-3}	1	1.23×10^{-3}	0.058	0.8173
	BC	5.38	1	5.38	252.79	< 0.0001
	A^2	4.40	1	4.40	206.55	< 0.0001
	B^2	3.66×10^{-3}	1	3.66×10^{-3}	0.17	0.6907
	C^2	1.59	1	1.59	74.67	< 0.0001
	Residual	0.15	7	0.021		
	Lack of fit	0.11	3	0.037	3.88	0.1116
	Pure error	0.038	4	9.53×10^{-3}		
	Cor total	109.09	16			
Contents of steroid saponins	Model	1792.80	9	199.20	53.03	0.0002
	A-extraction temperature	4.65	1	4.65	20.59	0.4731
	B-the ethanol concentration	1572.20	1	1572.20	326.98	< 0.0001
	C-solid-to-liquid ratio	192.57	1	192.57	29.45	0.0018
	AB	5.69	1	5.69	1.88	0.4295
	AC	0.034	1	0.034	5.23	0.9500
	BC	6.86	1	6.86	38.04	0.3876
	A^2	2.67	1	2.67	43.51	0.5836
	B^2	1.08	1	1.08	4.63	0.7259
	C^2	7.35	1	7.35	6.89	0.3723
	Residual	56.63	7	8.09		
	Lack of fit	44.86	3	14.95	5.08	0.0752
	Pure error	11.77	4	2.94		
	Cor total	1849.44	16			

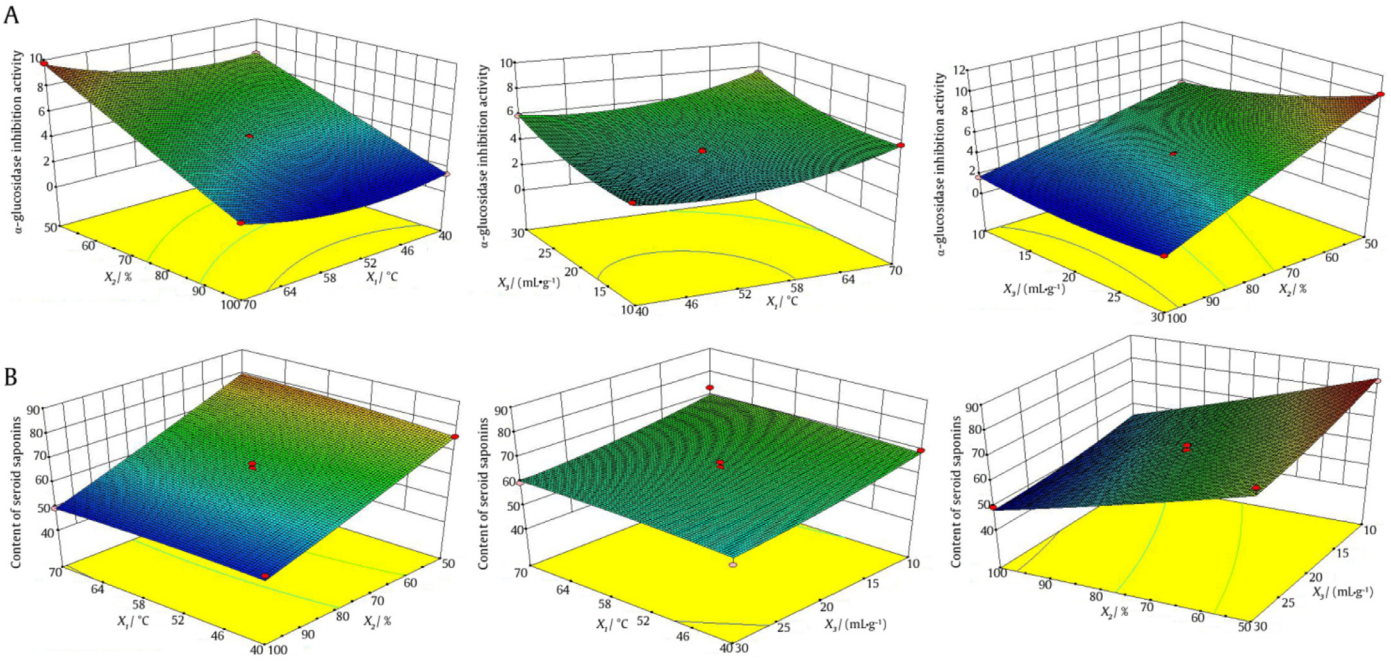

Fig. 2. Response surface plots (3D) of α-glucosidase inhibition activities (A) and contents of steroid saponins (B) as a function of significant interactions between factors: temperature, ethanol concentration, and liquid/solid ratio.

extraction temperature from 40 °C to 55 °C with liquid/solid ratio from 10:1 to 20:1 g/mL improved the inhibitory activities of α-glucosidase, while the activities did not continuously increase when extraction temperature and liquid/solid ratio exceeded 55 °C and 20:1. By carrying out parameter optimization based on α-glucosidase inhibitory activities, the optimal conditions for the extraction of α-glucosidase inhibitory activities constituents were as follow: extraction temperature 51.30 °C, ethanol concentration 100%, and liquid/solid ratio 23.02:1. Under these parameters, the predicted IC_{50} of α-glucosidase inhibitory activity was 0.94 mg/mL. Because the parameters are difficult to operate in the actual experiments, extraction temperature of 51 °C, concentration of ethanol of 100% and liquid/solid ratio of 23:1 were selected. The contents of steroid saponins decreased with increasing concentration of ethanol. The optimal conditions for the contents of steroid saponins were as follow: extraction temperature 62.78 °C, ethanol concentration 50.16%, and liquid/solid ratio 10.27:1.

3.3. Verification of models

In order to verify the suitability of the predicted response values, verification experiments were performed under the optimized conditions of α-glucosidase inhibitory activities in three replicates. The observed IC_{50} of α-glucosidase inhibitory activity was 0.96 mg/mL, which was very close to the predicted value. This indicated that the established quadratic models were statistically reliable and reasonable.

3.4. Identification of active fraction and structure characterization

The powders (20.0 g) of *A. asphodeloides* were extracted under the optimized conditions. The extract was applied to a D-101 macroporous resin column. It eluted with ethanol and water to afford 0%, 20%, 40%, 60%, 80%, and 100% ethanol fractions. It indicated that the extract was partitioned into six fractions and active compounds were gathered into 80% ethanol fraction. The results were summarized in Table 3.

Table 3
α-glucosidase inhibitory activities of 0%, 20%, 40%, 60%, 80%, and 100% ethanol fractions (mean ± SD, $n = 3$).

Samples	IC_{50} /(mg·mL^{-1})
0% fraction	1.89 ± 0.02
20% fraction	3.95 ± 0.03
40% fraction	0.34 ± 0.02
60% fraction	0.33 ± 0.01
80% fraction	0.05 ± 0.01
100% fraction	1.22 ± 0.02
Positive control	1.34×10^{-2} ± 0.03

As summarized in Table 4, a total of 25 saponins (Fig. 3) from the 80% ethanol fraction were identified and tentatively characterized.

To get the information about precursor ions and characteristic fragment ions of the compounds, timosaponin AIII, timosaponin BII, anemarrhenasaponin III, timosaponin G and anemarrhenasaponin I were injected into the LC-MS system. The standards have different structures and showed various fragment ions, they were classified into two types: furostanol glycosides (type I) and spirostanol glycosides (type II). The fragmentation patterns of timosaponin AIII and timosaponin BII were discussed in detail below.

Timosaponin AIII produced a precursor ion $[M+H]^+$ at *m/z* 741.4454 ($C_{39}H_{65}O_{13}$), The ions at *m/z* 579.3913 ($C_{33}H_{55}O_8$) and 417.3381 ($C_{27}H_{45}O_3$) were attributed to eliminate one glucosyl residue and one galactosyl residue. The ion at *m/z* 399.3269 ($C_{27}H_{43}O_2$) was produced by further neutral loss of H_2O. The fragment ion at *m/z* 273.2220 ($C_{19}H_{29}O$) was attributed to a skeleton residue, and then the ion continued to lose a molecule of H_2O to yield an ion at *m/z* 255.2120 ($C_{19}H_{27}$).

Timosaponin BII produced $[M+H-H_2O]^+$ at *m/z* 903.4953 ($C_{45}H_{75}O_{18}$) for its active site of C22 position. It could generate ions at *m/z* 741.4449, 579.3945, and 417.3430 by neutral loss of a glucose moiety from the C26 position and successive losses of ter-

Table 4
UPLC-Q-TOF-MS analysis for accurate mass measurements of constituents in 80% ethanol fraction.

No.	T_R / min	Formular	[M+COOH]$^-$	Fragment ions in positive ion (+) mode	Identification
1	3.08	$C_{45}H_{76}O_{20}$	981.4851	919, 757, 595, 433, 415, 289, 271	Timosaponin N
2	3.36	$C_{45}H_{76}O_{20}$	981.4862	919, 757, 595, 433, 415, 271, 253	25R-timosaponin N
3	3.42	$C_{45}H_{74}O_{19}$	963.4754	901, 739, 723, 577, 415, 255	Timosaponin M
4	3.61	$C_{45}H_{76}O_{19}$	965.4910	903, 741, 579, 435, 417, 399, 285, 273, 255	Timosaponin BII
5	3.92	$C_{45}H_{76}O_{19}$	965.4880	903, 741, 579, 435, 417, 399, 285, 273, 255	25R-timosaponin BII
6	4.05	$C_{44}H_{74}O_{18}$	935.4798	873, 711, 579, 549, 417, 399, 273, 255	Trigoneoside IIa
7	4.49	$C_{39}H_{64}O_{14}$	801.4258	739, 577, 415, 273, 255	Timosaponin G
8	4.53	$C_{39}H_{64}O_{15}$	817.4203	773, 611, 593, 449, 431, 413, 395, 289, 271	Timosaponin F
9	4.78	$C_{45}H_{76}O_{19}$	947.4808	903, 741, 579, 435, 417, 399, 273, 255	Anemarsaponin C
10	5.15	$C_{39}H_{64}O_{14}$	801.4249	757, 739, 595, 577, 433, 415, 273	Isomer of timosaponin G
11	5.59	$C_{39}H_{64}O_{14}$	801.4246	757, 739, 577, 433, 415, 255	Isomer of timosaponin G
12	5.85	$C_{39}H_{64}O_{14}$	801.4262	757, 595, 577, 433, 415, 273	Isomer of timosaponin G
13	6.16	$C_{39}H_{66}O_{14}$	803.4423	741, 579, 417, 271, 253	Anemarrhenasaponin I
14	6.60	$C_{39}H_{64}O_{14}$	801.4278	757, 739, 595, 433, 415, 271, 253	Anemarrhenasaponin A_2
15	6.85	$C_{39}H_{64}O_{14}$	801.4275	757, 739,595, 433, 415, 271, 253	25R- anemarrhenasaponin A_2
16	7.11	$C_{39}H_{62}O_{14}$	799.4116	755, 593, 575, 431, 413, 271	25(27)-ene-anemarrhenasaponin A_2
17	7.42	$C_{39}H_{64}O_{14}$	801.4281	757, 595, 433, 415, 271, 253	Anemarrhenasaponin III
18	8.30	$C_{39}H_{64}O_{13}$	785.4311	741, 579, 417, 399, 285, 273, 255	Isomer of timosaponin AIII
19	8.43	$C_{45}H_{74}O_{17}$	931.4834	887, 725, 579, 417, 399, 381, 273, 255	Rhamnosyl-timosaponin AI
20	8.65	$C_{39}H_{64}O_{13}$	785.4313	741, 579, 435, 417, 399, 273, 255	Isomer of timosaponin AIII
21	9.12	$C_{39}H_{64}O_{13}$	785.4315	741, 579, 399, 273,255	Timosaponin AIII
22	9.68	$C_{45}H_{74}O_{18}$	947.4790	903, 741, 579, 435, 417, 399, 273, 255	Isomer of anemarsaponin C
23	10.50	$C_{38}H_{62}O_{12}$	755.4216	711, 549, 417, 399, 273, 255	Xylosyl-glucosyl-sarasasapogenin
24	11.63	$C_{33}H_{54}O_8$	623.3842	579, 435, 273, 255	Timosaponin AI
25	12.06	$C_{33}H_{54}O_8$	623.3840	579, 435, 417, 399, 273, 255	Isomer of timosaponin AI

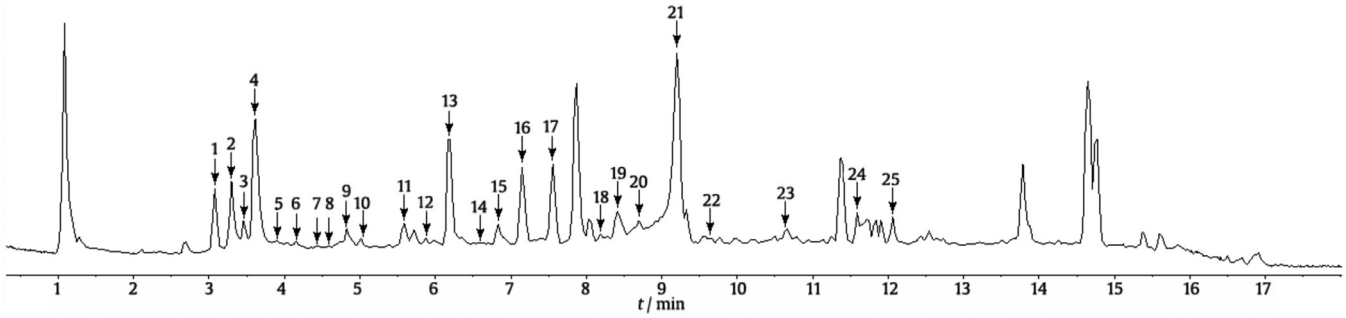

Fig. 3. Total ion chromatogram of 80% ethanol fraction in negative ion mode.

minal hexose of C3 position. The fragment ions at *m/z* 273.2294 and 255.2190 were attributed by the cleavage of the C20–C22 and C17–C20 bonds due to the presence of a 1622-epoxy residue and further loss of one molecule of H_2O. Major fragmentations proposed for timosaponin AIII and timosaponin BII were shown in Fig. 4.

Based on the authentic standards, retention time, exact mass, fragment ions, and structures in the literatures (Kang Yu et al., 2012; Kang, Zhang et al., 2012; Kang et al., 2013; Li, Zhou, Wu, & Ding, 2006; Pang et al., 2012; Youn et al., 2009; Zhang et al., 2006; Zhu, Guo, Fu, Zhang, & Liang, 2010), 25 compounds from the 80% ethanol fraction were deduced as follows. Parts of compounds from 80% fraction were shown in Fig. 5.

3.4.1. Characterization of peaks 1–6 and 13 of type I

These compounds were furostanol glycosides.

In negative ion mode, peak 1 produced [M+HCOO]$^-$ ion at *m/z* 981.4851 with the retention time of 3.08 min. Peak 1 presented [M+H−H_2O]$^+$ ion with mass accuracy at *m/z* 919.4902 in positive ion mode. It produced fragment ions at *m/z* 757.4370 [M+H−162]$^+$, 595.3873 [M+H−H_2O−2 × 162]$^+$, 433.3339 [M+H−H_2O−3 × 162]$^+$ and 415.3227 [M+H−2H_2O−3 × 162]$^+$, which were attributed to the sequential losses of one galactosyl, two glucosyls and two molecules of H_2O. Moreover, it was noteworthy that the fragment ion at *m/z* 271.2087 [415−$C_8H_{16}O_2$]$^+$ originating from the elimination of E-ring was observed in the MS/MS spectrum. Based on the fragment ions, it was tentatively identified as timosaponin N.

Peak 2 had the same molecular formula and similar fragmentation behavior as peak 1 with retention time of 3.36 min. Steroidal saponins with 25R configuration showed longer retention time than those with 25S configuration on a C_{18} column (Sun et al., 2014). Thus, it was tentatively identified as 25R-timosaponin N.

Peak 3 produced [M+HCOO]$^-$ ion at *m/z* 963.4754 at the retention time with 3.40 min in negative ion mode. In positive ion mode, the major fragment ions at *m/z* 901.4807 [M+H−H_2O]$^+$, 739.4279 [M+H−H_2O−162]$^+$, 577.4325 [M+H−H_2O−2 × 162]$^+$, 415.3241 [M+H−H_2O−3 × 162]$^+$, 273.2261 [M+H−H_2O−3 × 162−$C_8H_{14}O_2$]$^+$, and 255.2146 [M+H−2 × H_2O−3 × 162−$C_8H_{14}O_2$]$^+$ could be attributed to losses of one molecule of water, three hexosyl residues, one formula $C_8H_{14}O_2$, and another molecule of water. It was tentatively identified as timosaponin M.

Peak 4 was identified as timosaponin BII according to the standard.

Peak 5 had the same molecular formula and similar fragmentation behavior as peak 4. It was tentatively identified as 25R-timosaponin BII.

Peak 6 gave [M−H]$^-$ ion at *m/z* 889.4737 and [M+HCOO]$^-$ ion at *m/z* 935.4798 with the retention time of 4.03 min in negative ion mode. In positive ion mode, it produced major ion at *m/z* 873.4857 [M+H−H_2O]$^+$. The fragment ions at m/z 711.4225

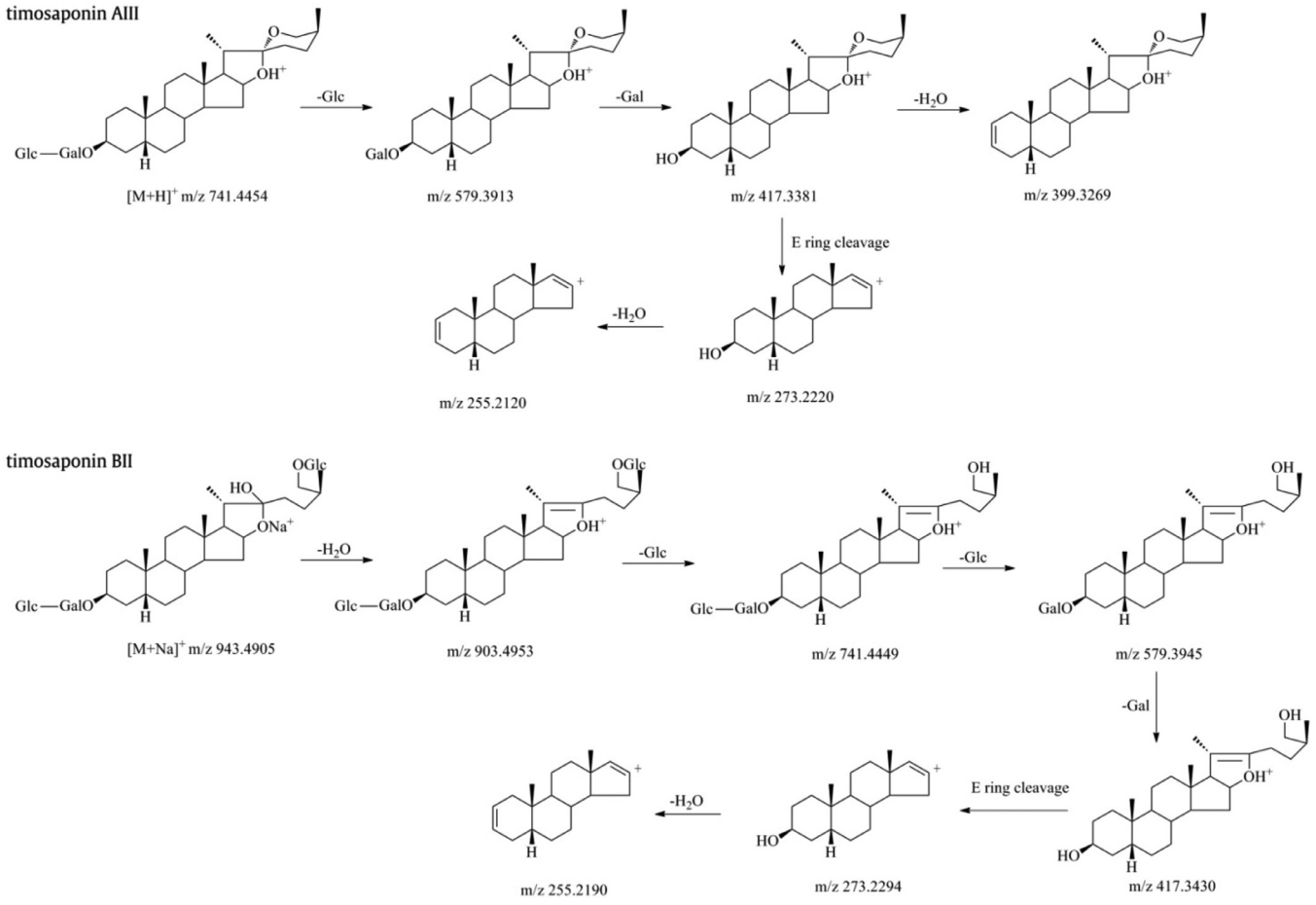

Fig. 4. Major fragmentations proposed for timosaponin AIII and timosaponin BII.

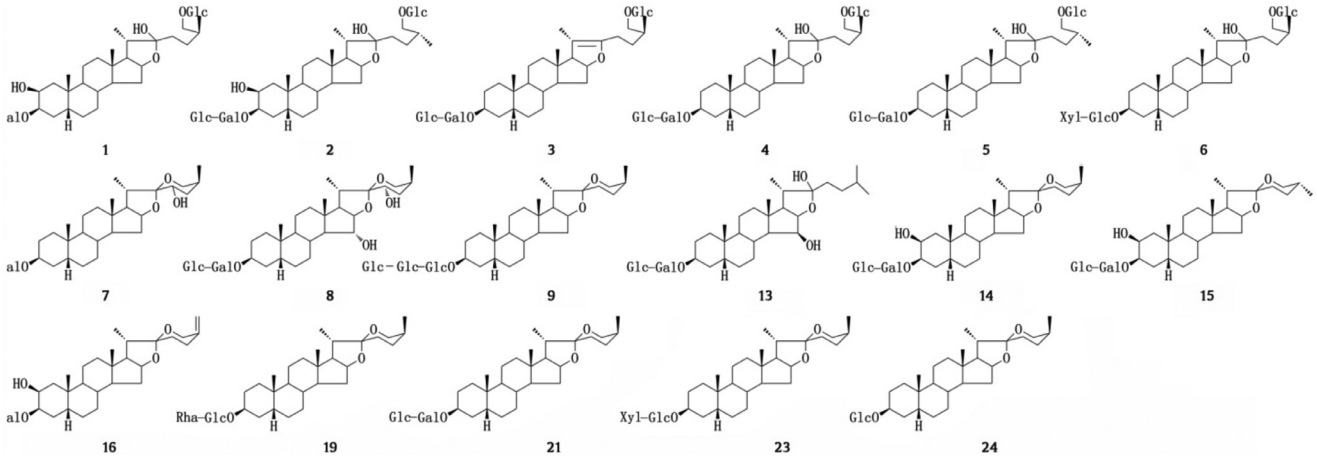

Fig. 5. Part of compounds from 80% ethanol fraction.

$[M+H-H_2O-162]^+$, 579.3958 $[M+H-H_2O-162-132]^+$, 549.3812 $[M+H-H_2O-2\times162]^+$, and 417.3381 $[M+H-H_2O-2\times162-132]^+$ indicted the pentosyl and hexosyls were the terminal glycones. Based on the diagnostic ions (273.2256 and 255.2144), peak 6 was tentatively identified as trigoneoside IIa.

Peak 13 showed the retention time of 6.16 min. It was identified as anemarrhenasaponin I according to the standard.

3.4.2. Characterization of peaks 7–12 and 14–25 of type II

These compounds were furostanol glycosides.

Peak 7 produced $[M-H]^-$ ion at *m/z* 755.4210 and $[M+HCOO]^-$ ion at *m/z* 801.4258 with the retention time of 4.47 min in negative ion mode. In positive ion mode, the molecular mass was 16 Da heavier than that of timosaponin AIII. It produced ions at *m/z* 739.4288 $[M+H-H_2O]^+$, 577.3752 $[M+H-H_2O-162]^+$, and 415.3221 $[M+H-H_2O-2\times162]^+$, which were corresponded to skeleton residues by successive losses of water and terminal glycones. Furthermore, the fragment ion at *m/z* 273.2233 was attributed to a skeleton residue by the cleavage of E-ring, and then the ion continued to lose H_2O to yield an ion at *m/z* 255.2170

$[273.2233-H_2O]^+$. It was identified as timosaponin G according to the standard.

Peak 8 produced $[M+HCOO]^-$ ion at *m/z* 817.4203 with the retention time of 4.50 min in negative ion mode. In positive ion mode, it produced prominent $[M+NH_4]^+$ and $[M+H]^+$ ions at *m/z* 790.4590 and 773.4405. The molecular mass was 32 Da heavier than that of timosaponin AIII. It produced fragment ions at *m/z* 611.3863 $[M+H-162]^+$, 593.3738 $[M+H-H_2O-162]^+$, 449.3300 $[M+H-2\times162]^+$, 431.3200 $[M+H-H_2O-2\times162]^+$, 413.3121 $[M+H-2H_2O-2\times162]^+$, and 395.2979 $[M+H-3H_2O-2\times162]^+$. Moreover, it was noteworthy that the fragment ion at *m/z* 289.2229 originating from elimination of the E-ring was observed in the MS/MS spectrum. The ions continued to lose H_2O to yield ions at *m/z* 271.2076 $[289.2229-H_2O]^+$ and 253.1950 $[271.2076-H_2O]^+$. It was tentatively identified as timosaponin F.

Peak 9 produced $[M-H]^-$ ion at *m/z* 901.4756 and $[M+HCOO]^-$ ion at *m/z* 947.4808 with the retention time of 4.79 min in negative ion mode. In positive ion mode, it produced prominent $[M+H]^+$ ion at *m/z* 903.4953, which could generate ions at *m/z* 741.4424 $[M+H-162]^+$, 579.3911 $[M+H-2\times162]^+$, 417.3396 $[M+H-3\times162]^+$, 399.3286 $[M+H-H_2O-3\times162]^+$, 273.2247 $[417.3396-C_8H_{16}O_2]^+$ and 255.2139 $[273.2247-H_2O]^+$. It was tentatively identified as anemarsaponin C or its isomer.

Peaks 10, 11 and 12 showed the same molecular formulas and similar fragmentation behaviors as peak 7. Thus, they were tentatively identified as the isomers of timosaponin G.

Peak 14 gave $[M-H]^-$ ion at *m/z* 755.4234 and $[M+HCOO]^-$ ion at *m/z* 801.4278 with the retention time of 6.64 min in negative ion mode. In positive ion mode, it produced $[M+NH_4]^+$ and $[M+H-H_2O]^+$ ions at *m/z* 774.4641 and 739.4303. The fragment ions at *m/z* 595.3877 $[M+H-162]^+$, 433.3354 $[M+H-2\times162]^+$, 415.3244 $[M+H-H_2O-2\times162]^+$ and 397.3147 $[M+H-2\times H_2O-2\times162]^+$ were attributed to the sequential losses of one galactosyl, one glucosyl and H_2O. Based on the diagnostic ions 289.2222 and 271.2101, it was tentatively identified as anemarrhenasaponin A_2.

Peak 15 gave $[M-H]^-$ ion at *m/z* 755.4229 and $[M+HCOO]^-$ ion at *m/z* 801.4275 with the retention time of 6.86 min in negative ion mode. It showed the same molecular formula and similar fragmentation behavior as peak 14. Thus, peak 15 was tentatively identified as the isomer of 25R-anemarrhenasaponin A_2.

Peak 16 gave $[M+HCOO]^-$ ion at *m/z* 799.4116 with the retention time of 7.18 min in negative ion mode. In positive ion mode, it produced $[M+NH_4]^+$ and $[M+H]^+$ ions at *m/z* 772.4545 and 755.4187. The fragment ions at m/z 593.3709 $[M+H-162]^+$, 575.3475 $[M+H-H_2O-162]^+$ and 413.3068 $[M+H-H_2O-2\times162]^+$ were attributed to the sequential losses of one galactosyl, H_2O and one glucosyl. Based on the diagnostic ion (271.2093), peak 16 was tentatively identified as 25(27)-ene-anemarrhenasaponin A_2.

Peak 17 produced $[M-H]^-$ ion at *m/z* 755.4232 and $[M+HCOO]^-$ ion at *m/z* 801.4281 with the retention time of 7.43 min in negative ion mode. In positive ion mode, it produced ions at m/z 774.4626 $[M+NH_4]^+$ and 757.4422 $[M+H]^+$. The fragment ions at *m/z* 595.3849 $[M+H-162]^+$, 433.3340 $[M+H-2\times162]^+$ and 415.3236 $[M+H-H_2O-2\times162]^+$ were attributed to the sequential losses of one galactosyl, one glucosyl and H_2O. Based on the diagnostic ion (289.2197, 271.2089, and 253.1977), it was identified as anemarrhenasaponin III according to the standard.

Peak 18 gave $[M+HCOO]^-$ ion at *m/z* 785.4311with the retention time of 8.31 min in negative ion mode. In positive ion mode, it produced $[M+NH_4]^+$ and $[M+H]^+$ ions at *m/z* 758.4951 and 741.4432. The fragment ions showed similar fragmentation behavior as timosaponin AIII. Thus, it was tentatively identified as the isomer of timosaponin AIII.

Peak 19 produced $[M+HCOO]^-$ ion at *m/z* 931.4834 with the retention time of 8.44 min in negative ion mode. In positive ion mode, it produced $[M+NH_4]^+$ and $[M+H]^+$ ions at *m/z* 904.5229 and 887.4978. The major fragment ions at *m/z* 725.4512, 579.3909, 417.3384, 399.3277, 273.2236, and 255.2137 could be attributed to losses of one rhamanopyranosyl residue, one hexosyl residue, one molecule of water, one formula of $C_8H_{14}O_2$ and another molecule of water. It was tentatively identified as rhamnopyranosyl-timosaponin AI.

Peak 20 with the retention time of 8.51 min showed the same formula and similar fragmentation behavior as timosaponin AIII. Thus, it was tentatively identified as the isomer of timosaponin AIII.

Peak 21 was definitely identified as timosaponin AIII according to the standard.

Peak 22 produced $[M+HCOO]^-$ ion at *m/z* 947.4790 with the retention time of 9.67 min in negative ion mode. In positive ion mode, it produced $[M+NH_4]^+$ and $[M+H]^+$ ions at *m/z* 920.5253 and 903.4906. The major fragment ions at *m/z* 741.4504, 579.3906, 417.3401, 399.3288, 273.2241, and 255.2153 could be attributed to losses of three hexosyl residues, one molecule of water, one formula $C_8H_{14}O_2$ and another molecule of water. It was identified as anemarsaponin C or its isomer.

Peak 23 gave $[M+HCOO]^-$ ion at *m/z* 755.4216 with the retention time of 10.50 min in negative ion mode. In positive ion mode, it produced $[M+NH_4]^+$ and $[M+H]^+$ ions at *m/z* 728.4633 and 711.4327. The major fragment ions at *m/z* 549.3793, 417.3393, 399.3301, 273.2230, and 255.2132 could be attributed to losses of one pentosyl residue, one hexosyl residue, one molecule of water, one formula $C_8H_{14}O_2$ and another molecule of water. It was identified as the xylosyl-glucosyl-sarasasapogenin.

Peak 24 gave $[M+HCOO]^-$ ion at *m/z* 623.3842 with the retention time of 11.62 min in negative ion mode. In positive ion mode, it produced $[M+H]^+$ ion at *m/z* 579.3896. The major fragment ions were at *m/z* 435.2760, 273.2248 and 255.2132. It was identified as timosaponin AI or its isomer.

Peak 25 with the retention time of 12.03 min showed the same formula and similar fragmentation behavior as peak 24. Thus, it was tentatively identified as timosaponin AI or its isomer.

3.5. Influential priority of structures of compounds for α-glucosidase inhibitory activities

To get a better understanding on the influences of the structures of compounds for α-glucosidase inhibitory activities, grey relational coefficients and grey relational grades were calculated accordingly to show a comprehensive evaluation. The precision test was carried out by injecting the same sample solution 6 times for peak area of each analyte and retention time. It indicated that the analytical method was suitable for determination. Compounds **5, 10, 11, 12, 15, 18** and **20** were not calculated for their low contents. Grey relational orders were shown in Table 5. It can be seen that, regarding the results, the predicted α-glucosidase inhibitory activities of the compounds were **7** > **2** > **1** > **22** > **23** > **3** > **9** > **21** > **24** > **4** > **13** > **8** > **14** > **16** > **17** > **25** > **6** > **19**.

4. Discussion

In the single-factor experiments, ethanol concentration and the extraction temperature had more remarkable effects on α-glucosidase inhibition than liquid/solid ratio. RSM employing BBD was applied to test the optimal conditions for the extraction. 3D plots of the response surface for the inhibitory activities of α-glucosidase and the contents of steroid saponins showed that the activities did not increase with the increase of the

Table 5
Grey relational orders associated with compounds and α-glucosidase inhibitory activities.

Grey relational orders	Peak number	Grey relational index
1	7	0.7827
2	2	0.7821
3	1	0.7651
4	22	0.7376
5	23	0.7339
6	3	0.7338
7	9	0.7008
8	21	0.6996
9	24	0.6961
10	4	0.6949
11	13	0.6877
12	8	0.6812
13	14	0.6665
14	16	0.6632
15	17	0.6618
16	25	0.6556
17	6	0.6445
18	19	0.6188

contents of steroid saponins. In order to further discussed the structure-activity relationship, 20.0 g of *A. asphodeloides* were extracted under the optimal conditions according to the results of α-glucosidase inhibitory activities. The extract was applied to a D-101 macroporous resin column. It eluted with ethanol and water to give six ethanol fractions. It indicated that the active compounds were gathered into 80% ethanol fraction.

The compounds from 80% ethanol fraction were identified by UPLC-Q-TOF-MS. The data were obtained using Analyst TF 1.7.1 Software. PeakView, MasterView and MultiQuant™ Software were used to analyze the data. Both positive and negative ion modes were tested. The results showed that the analyses were obtained with the positive ion mode to obtain greater responses to fragments. The analyses were obtained with the negative ion mode to obtain high sensitivity of $[M+COOH]^-$. Using aqueous acetonitrile mobile phase with a small amount of acid could improve the peak shape of the components.

After analyzing the data, the compounds of this fraction were mainly consisted of steroid saponins. Steroid saponins of *A. asphodeloides* primarily composed of furostanol glycosides and spirostanol glycosides. The MS/MS fragmentation patterns of timosaponin AIII and timosaponin BII were discussed as examples. They would produce MS/MS ions by losing glycosyl residues, water and E-ring cleavage. If the ions at *m/z* 417, 255 and 273 were appeared, it suggested no hydroxyl attached to the A, B, C, and D rings. If the ions at *m/z* 433 and 415 were detected, there should be one hydroxyl group substituent on the A, B, C, or D rings. The type of glycosides, the kinds, number and connection orders of sugar moieties would affect the retention time. We used PeakView Software to simulate the fragmentation pattern of each compound. It can raise the reliability of the results. Peaks 19 and 23 were tentatively identified as new structures. It would be a guide for separating new compounds from *A. asphodeloides* in the future. However, the analytical method has some limitations in identifying the sugar residues and the linkage position of sugar moieties. To confirm the structures of the compounds, NMR experiments are necessary.

5. Conclusion

The rhizomes of *A. asphodeloides* had been reported to have α-glucosidase inhibitory activities. In order to find the α-glucosidase inhibitors, response surface methodology was applied to optimize conditions for the extraction of α-glucosidase inhibitory compounds. The extract was applied to a D-101 macroporous resin column. The fraction eluted by 80% ethanol showed the best inhibitory activity. Twenty-five steroid saponins were tentatively identified by UPLC-Q-TOF-MS. The structure-activity relationship was discussed based on grey relational analysis.

Conflict of interest

The authors declare that there are no conflicts of interest.

Acknowledgments

The authors are grateful to the financial supports from Qiqihar Civic Scientific and Technological Project (SFGG-201559).

References

Dou, F., Xi, M. M., Wang, J. X., Tian, X. R., Hong, L. J., Tang, H. F., & Wen, A. D. (2013). α-Glucosidase and α-amylase inhibitory activities of saponins from traditional Chinese medicines in the treatment of diabetes mellitus. *Pharmazie, 68*(4), 300–304.

Hirsh, A. J., Yao, S. Y., Young, J. D., & Cheeseman, C. I. (1997). Inhibition of glucose absorption in the rat jejunum: A novel action of α- D-glucosidase inhibitors. *Gastroenterology, 113*(1), 205–211.

Ji, X., & Feng, Y. F. (2010). Advances in studies on saponins in Anemarrhena as phodeloides. *Chinese Traditional and Herbal Drugs, 41*(4), 12–15 attach.

Joseph, B., & Jini, D. (2011). Insight into the hypoglycaemic effect of traditional indian herbs used in the treatment of diabetes. *Journal of Medicinal Plants Research, 5*(4), 352–376.

Ichiki, H., Takeda, O., Sakakibara, I., Terabayashi, S., Takeda, S., & Sasaki, H. (2007). Inhibitory effects of compounds from *Anemarrhenae Rhizoma* on α-glucosidase and aldose reductase and its contents by drying conditions. *Chinese Journal of Natural Medicines, 61*(2), 146–153.

Kang, L. P., Yu, K., Zhao, Y., Liu, Y. H., Yu, H. S., et al. (2012). Characterization of steroidal glycosides from the extract of *Paris polyphylla* var. *yunnanensis* by UPLC/Q-TOF MSE. *Journal of Pharmaceutical and Biomedical Analysis, 62*(25), 235–249.

Kang, L. P., Zhang, J., Cong, Y., Li, B., Xiong, C. Q., Zhao, Y., et al. (2012). Steroidal glycosides from the rhizomes of *Anemarrhena asphodeloides* and their antiplatelet aggregation activity. *Planta Medica, 78*(6), 611–616.

Kang, L. P., Zhao, Y., Pang, X., Yu, H. S., Xiong, C. Q., Zhang, J., et al. (2013). Characterization and identification of steroidal saponins from the seeds of *Trigonella foenum-graecum* by UPLC and hybrid TOF-MS. *Journal of Pharmaceutical and Biomedical Analysis, 74*(23), 257–267.

Kang, Y. J., Chung, H. J., Nam, J. W., Park, H. J., Seo, E. K., Kim, Y. S., et al. (2011). Cytotoxic and antineoplastic activity of timosaponin A-III for human colon cancer cells. *Journal of Natural Products, 74*(4), 701–706.

Khang, P. V., Phuong, D. M., & Ma, L. (2017). New steroids from *Anemarrhena asphodeloides* rhizome and their α-glucosidase inhibitory activity. *Journal of Asian Natural Products Research, 19*(12), 468–473.

Lee, B., Jung, K., & Kim, D. H. (2009). Timosaponin AIII, a saponin isolated from *Anemarrhena asphodeloides*, ameliorates learning and memory deficits in mice. *Pharmacology Biochemistry & Behavior, 93*(2), 121–127.

Li, R., Zhou, Y., Wu, Z. J., & Ding, L. S. (2006). ESI-QqTOF-MS/MS and APCI-IT-MS/MS analysis of steroid saponins from the rhizomes of *Dioscorea panthaica*. *Journal of Mass Spectrometry, 41*(1), 1–22.

Li, Y. J., Li, Q., He, F. Y., Ma, J., & Ma, K. S. (2014). Grey relational analysis on fingerprints of extracts from *Polygoni Cuspidati Rhizoma* et *Radix* and antioxidant capacity *in vitro*. *Chinese Journal of Experimental Traditional Medical Formulae, 20*(14), 76–80.

Martin, A. E., & Montgomery, P. A. (1996). Acarbose: An α-glucosidase inhibitor. *American Journal of Health-System Pharmacy, 53*(19), 2277–2290.

Nhiem, N. X., Kiem, P. V., Minh, C. V., Ban, N. K., Cuong, N. X., Tung, N. H., et al. (2010). Alpha-glucosidase inhibition properties of cucurbitane-type triterpene glycosides from the fruits of *Momordica charantia*. *Chemical and Pharmaceutical Bulletin, 58*(5), 720–724.

Nian, S. H., Li, H. J., Liu, E. H., & Li, P. (2017). Comparison of α-glucosidase inhibitory effect and bioactive constituents of *Anemarrhenae Rhizoma* and fibrous roots. *Journal of Pharmaceutical and Biomedical Analysis, 145*, 195–202.

Oh, S., Rheem, S., Sim, J., Kim, S., & Baek, Y. (1995). Optimizing conditions for the growth of *Lactobacillus casei* YIT 9018 in tryptone-yeast extract-glucose medium by using response surface methodology. *Applied and Environmental Microbiology, 61*(11), 3809–3814.

Pang, X., Kang, L. P., Yu, H. S., Zhao, Y., Xiong, C. Q., Zhang, J., et al. (2012). Rapid isolation of new furostanol saponins from fenugreek seeds based on UPLC coupled with a hybrid quadrupole time-of-flight tandem mass spectrometry. *Journal of Separation Science, 35*(12), 1538–1550.

Sun, C. P., Gao, W. P., Zhao, B. Z., & Cheng, L. Q. (2013). Optimization for preparation of lemon-catalyzed ginsenoside Rg3 by response surface method. *Chinese Herbal Medicines, 5*(3), 217–223.

Sun, Y., Li, L. G., Liu, C. T., Liu, Q. B., Li, L. Z., Peng, Y., et al. (2014). Two new components from the rhizome of *Anemarrhena asphodeloides* Bge. and their antiplatelet aggregative activity. *Phytochemistry Letters, 7*, 207–211.

Sun, Y., Liu, L. Y., Peng, Y., Liu, B. J., Lin, D. J., Li, L. Z., et al. (2015). Metabolites characterization of timosaponin AIII *in vivo* and *in vitro* by using liquid chromatography-mass spectrometry. *Journal of Chromatography B, 997*, 236–243.

Sun, Y., Peng, Y., Li, L. G., Zheng, L. W., Lin, D. J., Li, L. Z., et al. (2014). A platform for screening potential anticholinesterase fractions and components obtained from *Anemarrhena asphodeloides* Bge. for treating alzheimer's disease. *Evidence-Based Complementary and Alternative Medicine, 524650*, 1–11.

Sun, Y., Wu, J., Sun, X., Huang, X. X., Li, L. Z., Liu, Q. B., et al. (2016). Steroids from the rhizome of *Anemarrhena asphodeloides* and their cytotoxic activities. *Bioorganic & Medicinal Chemistry Letters, 26*, 3081–3805.

Toeller, M. (1994). Alpha-glucosidase inhibitors in diabetes: Efficacy in NIDDM subjects. *European Journal of Clinical Investigation, 24*(3), 31–35.

Wang, G. C., Peng, Z. Y., Wang, J., Li, J., & Li, X. (2016). Synthesis, biological evaluation, and molecular docking study of N-arylbenzo[d]oxazol-2-amines as potential alpha-glucosidase inhibitors. *Journal of Pharmaceutical and Biomedical Analysis, 24*(11), 5374–5379.

Wang, G. J., Lin, L. C., Chen, C. F., Cheng, J. S., Lo, Y. K., Chou, K. J., et al. (2002). Effect of timosaponin A-III, from *Anemarrhenae asphodeloides* Bunge (Liliaceae), on calcium mobilization in vascular endothelial and smooth muscle cells and on vascular tension. *Life Science, 71*(9), 1081–1090.

Wang, H. B., Qi, W., Zhang, L., & Yuan, D. (2014). Qualitative and quantitative analyses of alkaloids in *Uncaria* species by UPLC-ESI-Q-TOF/MS. *Chemical and Pharmaceutical Bulletin, 62*(11), 1100–1109.

Wang, N., Feng, Y. B., Zhu, M. F., Siu, F. M., Ng, K. M., & Che, C. M. (2013). A novel mechanism of XIAP degradation induced by timosaponin AIII in hepatocellular carcinoma. *Biochimica et Biophysica Acta, 1833*(12), 2890–2899.

Xu, H. Y., Li, K., Chen, Y. J., Zhang, Y. C., Tang, S. H., Wang, S. S., et al. (2013). Study on the absorbed fingerprint-efficacy of Yuanhu Zhitong Tablet based on chemical analysis, vasorelaxation evaluation and data mining. *Plos One, 8*(12) e81135/1–e81135/11.

Xu, J., Sheng, G. P., Luo, H. W., Fang, F., Li, W. W., Zeng, R. J., et al. (2011). Evaluating the influence of process parameters on soluble microbial products formation using response surface methodology coupled with grey relational analysis. *Water Research, 45*(2), 674–680.

Yang, K., Yu, Y., & Hwang, S. (2003). Selective optimization in thermophilic acidogenesis of cheese-whey wastewater to acetic and butyric acids: Partial acidification and methanation. *Water Research, 37*(10), 2467–2477.

Youn, U. J., Lee, Y. S., Jeong, H., Lee, J., Nam, J. W., Lee, Y. J., et al. (2009). Identification of antiadipogenic constituents of the rhizomes of *Anemarrhena asphodeloides*. *Journal of Natural Products, 72*(10), 1895–1898.

Zhang, J., Ma, B. P., Kang, L. P., Yu, H. S., Yang, Y., Yan, X. Z., et al. (2006). Furostanol saponins from the fresh rhizomes of *Polygonatum kingianum*. *Chemical and Pharmaceutical Bulletin, 54*(7), 931–935.

Zhao, Y., Kang, L. P., Yu, H. S., Zhang, J., Xiong, C. Q., Pang, X., et al. (2013). Structure characterization and identification of steroidal saponins from the rhizomes of *Anemarrhena asphodeloides* by UPLC and hybrid quadrupole time-of-flight mass spectrometry. *International Journal of Mass Spectrometry, 341-342*, 7–17.

Zhou, X. L., Liang, J. S., Zhang, Y., Zhao, H. D., Guo, Y., & Shi, S. Y. (2015). Separation and purification of α-glucosidase inhibitors from *Polygonatum odoratum* by stepwise high-speed counter-current chromatography combined with Sephadex LH-20 chromatography target-guided by ultrafiltration-HPLC screening. *Journal of Chromatography B, 985*, 149–154.

Zhu, J. B., Guo, X. J., Fu, S. P., Zhang, X. L., & Liang, X. M. (2010). Characterization of steroidal saponins in crude extracts from *Dioscorea zingiberensis* C. H. Wright by UPLC-ESI-Q-TOF-MS. *Journal of Pharmaceutical and Biomedical Analysis, 53*(3), 462–474.